Influence of plane wave cut-off on structural and electronic properties in Sn-BEA and Ti-BEA zeolite water molecule interaction

Bhakti S. Kulkarni [a], Sailaja Krishnamurty [b], Sourav Pal [a],*

[a] Physical Chemistry Division, National Chemical Laboratory, Pune 411 008, India
[b] Electrochemical Research Institute (CECRI), Karaikudi 630 006, India

ABSTRACT

Periodic systems are best described by the pseudo-potential methods. However, the accuracy of its description depends on the cut-off of plane wave basis. This is much more critical in the case of weak interactions, where a clear understanding on the influence of plane wave cut-off on the structural and electronic properties is not readily available in the literature. In the present work, we have taken a metal substituted beta zeolite–H_2O complex for understanding this objective. Our studies show that while a lower cut-off of 500 eV is sufficient for the convergence of the structural parameters, description of energy-dependent properties necessitates a high cut-off value.

© 2009 Elsevier B.V. All rights reserved.

1. Introduction

Among several theoretical methods, the total energy techniques such as Hartree–Fock (HF) and post-HF methods have been successfully applied to understand the structure and properties of systems containing 10–100 electrons [1]. The advances in density functional theory (DFT) [2,3] have facilitated the extension of these studies to large polyatomic molecules with more than 100 electrons. With the advent of pseudo-potential (PP) based DFT methods [4], these studies were extended to periodic systems where core electrons are represented by pseudo-potentials and valence electrons are dealt with plane waves (PW). This reduces the computational expense of simulation [5] in dealing with large complex molecules and, in particular, for periodic systems. In addition, PW technique is popular as it is straight forward to use in solid state periodic simulations. PW periodic DFT (p-DFT) based methods have found an impressive range of applications [6–10].

An extremely appealing feature of PW basis is that the energies calculated do not suffer from the basis set superposition error (BSSE). This enables a better description of adsorption processes that are characterized by interaction energies of moderate strength. However, the quality of the PW basis set is specified by an important parameter: the electronic kinetic energy cut-off, E_{cut}. Therefore, with a given structure and a set of pseudo-potentials, the first task in any PW calculation is to choose appropriate cut-off energy for the basis. This is done by means of a convergence test, in which calculations are carried out at a series of increasing cut-off energies. The convergence of a given quantity, usually the

total energy, is monitored towards its large cut-off limit. However, as will be discussed later, this is not a sufficient test for studying weak interactions.

Many physical properties such as bulk moduli, piezoelectric constant, phonon, and phase transitions, are related to the total energy of a system. In contrast, chemical properties such as interaction energy, adsorption energy, intrinsic reaction barriers etc., are related to the differences in total energies of two systems. In p-DFT, truncation of PW at a finite cut-off may lead to an error in the calculation of the total energy and other energy-related properties. These errors are usually reduced by increasing the value of kinetic energy cut-off and hence the number of PW. In principle, the PW cut-off is increased until the calculated total energy is converged. However, a relative property, such as weak interaction energy need not converge at the same rate as that of the total energy. Hence, all these parameters, despite having some default values in the program, need to be carefully chosen in a given simulation.

Based on the above issues and inspired by the work of Ramirez-Solis and co-workers [11], we examine the convergence of total and interaction energies as a function of PW basis. In the latter work the statistical and dynamical structure, energy convergence, and frequency convergence of Hydrogen Fluoride clusters were studied using standard norm conserving pseudo-potentials. The authors enclosed each molecular cluster in a box of 15 Å. Here the vacuum region and the decaying wave functions are more delicate to handle with plane waves and the cut-off is crucial. Their study verified the need of a large plane wave cut-off for a proper description of ionic and hydrogen bonded interactions in a cluster. The authors mentioned that it would be interesting to have similar comparisons with the ultrasoft pseudo-potentials. It is to be noted

* Corresponding author.
E-mail address: s.pal@ncl.res.in (S. Pal).

that in the present study, we have used ultrasoft pseudo-potentials, which are known to typically require 2.5–4 times lower cut-offs. Although similar attempts [12–17] have been previously made in the computational chemistry community, a clear description of the PW variation for a large periodic model is not yet available.

Consequently, we aim to examine the influence of PW cut-off on the convergence of a weakly interacting zeolite and water complex. These catalysts are so chosen because they are preferentially hydrophobic in nature [18,19]. In addition, zeolite beta (BEA) is a well known active catalyst for carrying out several organic reactions. Hence, the nature of its interaction, which is mainly weak attractive and coordinative, with several organic reagents and reaction media necessitates an understanding using such theoretical studies [20–22]. The incorporation of Ti- and Sn- at active sites (T-sites) finely tunes acidity and increases activity of the BEA (T-BEA). Several studies describe the structural and energetic features of these systems [23–27]. Structural details of Sn/Ti-BEA-complexes, their cohesive energies, interaction energies along with reactivity are well studied in the literature [22,28–34]. This system is an appropriate example as it features a rigid and flexible framework with a simultaneous presence of two types of bonding, a covalent one e.g. Si–O and a weak hydrogen bonding due to the adsorption of a water molecule, representing a wide range of chemical systems. Hence, the main focus of present study will be to examine the role of PW in describing the structural properties such as bond length, bond angle etc., total energies of each individual system and their respective interaction energies. We also include a short discussion on the density-dependent HOMO, LUMO and ELF contours. These maps are calculated at PW cut-offs of 500 eV and 1000 eV to highlight the effect of basis extension.

2. Simulation model

Since the zeolites are periodic and crystalline, their simulation is a challenging task. The most appreciated approximation for investigation of active sites within zeolites is a computationally cheap cluster model [35–38] approach. However, since a cluster model is an abbreviated form of a 3D structure, it introduces some artificial surface states and does not consider the long range interactions. In addition, the presence of a few substituted active sites in zeolites forces one to use periodic boundary conditions (PBC) in their representation. PBC corresponds to one or more unit cells replicated to form an infinite lattice. This ensures that the density of the system remains constant throughout the simulation and that the surface effects are absent. Despite the complexity to build such models, several reaction mechanisms of these catalytic materials are studied periodically [39–41]. However, as mentioned above, a clear understanding on the convergence of structure and energy with respect to PW cut-off is not available in the literature.

The unit cell of an ideal fully siliceous BEA zeolite consists of 192 atoms with 64 Si and 128 O atoms distributed within the tetragonal lattice of dimensions $12.6 \text{ Å} * 12.6 \text{ Å} * 26.2 \text{ Å}$. Fig. 1 shows the unit cell of BEA zeolite. There are nine distinct crystallographically defined T-sites. We adopt the structure of BEA from our earlier theoretical study [34] and incorporate the Sn- and Ti-atoms at T2 and T1 sites [42], respectively. The interaction of H_2O molecule at the active site is very important since it gives rise to geometric perturbations and energetic differences. Schematic representation of T-BEA/H_2O is given in Fig. 1 (small molecule adsorbed on T-site). The most favorable H_2O ligand approach at the active T-site is along the b axis. Various other possible orientations of H_2O ligand at the active site result in high energy and high force values. The insertion of water molecule results in elongation of one of the T–O bonds compared to that of the others present in TO_4
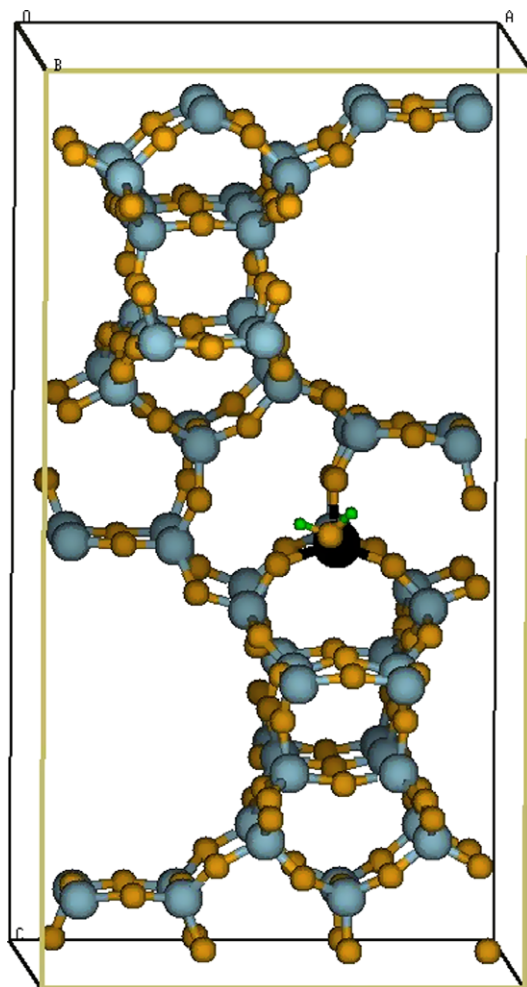

Fig. 1. Optimized T-BEA unit cell with interaction of H_2O molecule at T1 site. Black sphere, Ti-atom; gray spheres, Si atoms; yellow spheres, O atoms; and small green spheres, H atoms. (For interpretation of the references to colour in this figure legend, the reader is referred to the web version of this article.)

unit. The four framework oxygen atoms are no longer equivalent and split into one axial ($T–O_{ax}$) opposite to the adsorbed ligand and three equatorial ($T–O_{eq}$), respectively. Consequently, six O–T–O angles of the TO_4 unit give rise to two triplets, $O_{eq}–T–O_{eq}$ and $O_{eq}–T–O_{ax}$. These are labeled as α and β, respectively. This geometric distortion leading to more distorted bipyramidal geometry makes the structure more reactive.

3. Computational details

All periodic calculations in the present study are carried out using VASP [9,10]. The PBC facilitates one to add long range electrostatic interactions through Ewald summations. As in standard DFT programs, the stationary ground state in p-DFT is calculated by solving iterative Kohn–Sham equations. We use Vanderbilt's ultrasoft pseudo-potentials [43] for describing the behavior of core electrons. Here we vary the number of PW for valence, and analyze the properties of the systems with respect to their number. The energy cut-off for plane waves is varied from 300 eV i.e. 21.83 Ry to 1200 eV i.e. 88.20 Ry. The exchange–correlation functional is expressed by the generalized gradient approximation (GGA) using Perdew–Wang 91 [44] functional. The calculations are restricted to gamma point in the Brillouin zone sampling. The structural optimization of Sn- and Ti-BEA is carried out using the conjugate gradient method. The structure is considered to be optimized when
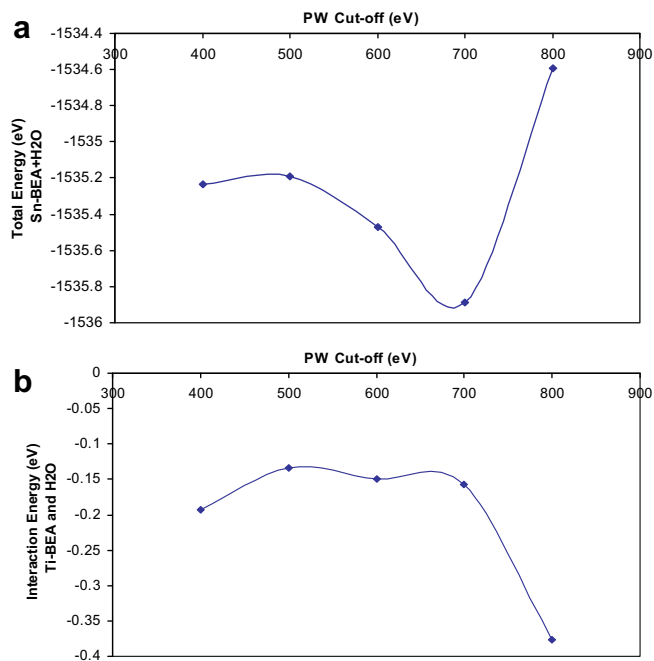
Fig. 2. (a) Total energy of Sn-BEA + H$_2$O as a function of PW cut-off at default FFT grid. (b) Interaction energy of Ti-BEA and H$_2$O as a function of PW cut-off at default FFT grid.

Fig. 3. Ti-BEA nuclear–nuclear repulsion energy (Ewald energy) (eV) as a function of PW cut-off (eV).

Fig. 4. H$_2$O total energy (eV) as a function of PW cut-off (eV).

the maximum force on each atom is less than 0.08 eV/Å. Similar optimization procedures are repeated for the interaction of water molecule at Sn- and Ti-centers in BEA, and for that of periodic bare H$_2$O molecule. The above procedure of optimization is followed for all systems with PW cut-off varying from 300 eV to 1200 eV at an interval of 100 eV.

While calculating the total energy, one should take care of the charge density. The charge density is computed easily in real space, as it is simply the square of magnitude of the wave function. However, the charge density has components up to twice the cut-off wave vector in case of PW. Most programs assign some default grid size according to the need of the computation. However, the accuracy of such default values cannot be taken as granted for systems where a large number of PWs are required to explain weak interactions. As an illustration, Fig. 2a shows a model convergence pattern of the total energy of Sn-BEA and H$_2$O complex as a function of cut-off at default FFT grid assigned by the VASP program. Similarly, the total energy of each system converge smoothly until 700 eV cut-off, beyond which it fails to converge with default grid values. A consequence of this is also observed in the respective interaction energy. The Fig. 2b highlights the oscillatory interaction energies of the complexes as a result of bad convergence of the total energy of the individual system. As the energy-dependent relative property is far from the convergence, it is necessary to explore the energy surface of materials using higher cut-offs. Hence, to maintain a faithful representation of charge density one must compute it on a grid twice denser than that required in the representation of the wave function. In addition, considering the size of our periodic model and to achieve a better relative accuracy, we fix the FFT grid to a cubical 96 * 96 * 96 * mesh size. Further discussion of the results will be mostly in graphical form. The graphical figures are obtained from differential plots, where, we assume the converged values at limiting cut-off (1000 eV) as a reference zero and rest of the higher energies are subtracted from these reference values. Fig. 3, taken as evidence for structural convergence, depicts nuclear–nuclear repulsion energy as a function of cut-off. Fig. 4 gives the total energy of water as a function of cut-off. Fig. 5a and b depicts
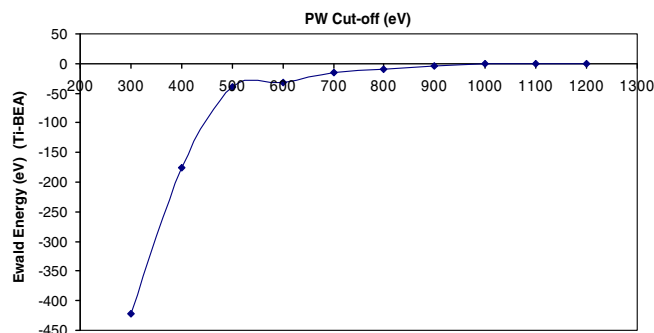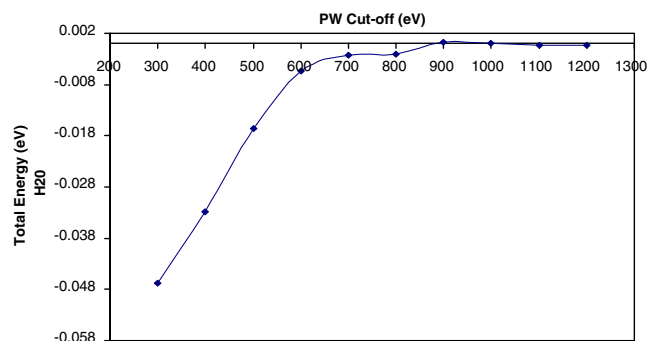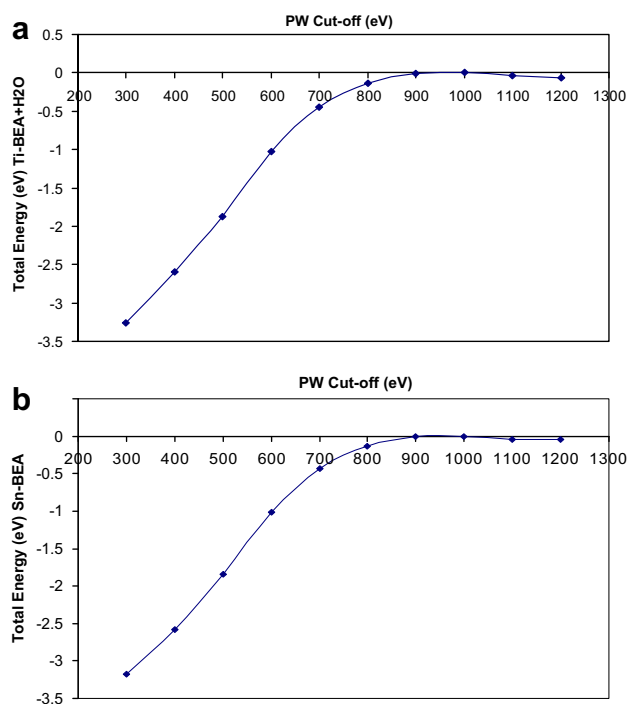

Fig. 5. (a) Ti-BEA + H$_2$O total energy (eV) as a function of PW cut-off (eV). (b) Sn-BEA total energy (eV) as a function of PW cut-off (eV).

the total energy convergence plots of Ti-BEA–H$_2$O complex and Sn-BEA, respectively. The rest of the systems follow similar trend of
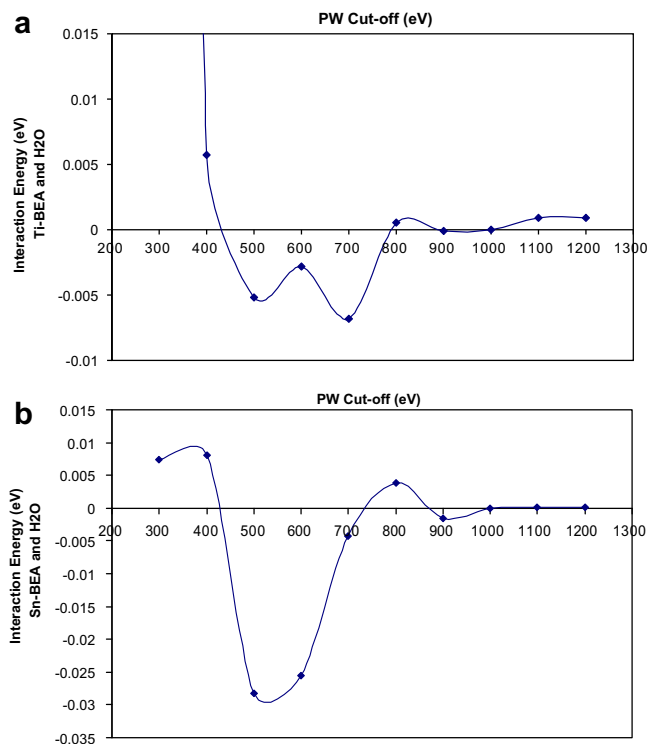
Fig. 6. (a) Ti-BEA and H_2O Interaction energy (eV) as a function of PW cut-off (eV). (b) Sn-BEA and H_2O Interaction energy (eV) as a function of PW cut-off (eV).

the convergence. We have not presented figures for them. Fig. 6a and b displays the most important property, the fluctuations of interaction between Ti-BEA and Sn-BEA with water molecule, respectively.

4. Results and discussion: role of plane wave cut-off in structural and energy convergence

We first examine the convergence of structural parameters over the range of PW cut-off, 300–1200 eV. Table 1 shows the convergence of some relevant geometrical parameters. The intra-molecular distances are quite stable from 400 eV. As a result of water adsorption, both the T-BEA–water adducts show an elongation of all T–O bond lengths as compared to the bare T-BEA systems. For Sn-BEA, it is stable at 1.91 Å, where as in water adduct, it gets elongated to 1.92 Å. For Ti-BEA, T–O distance converges to 1.80 Å. This gets elongated and converges to 1.82 Å in its water adduct. In T-BEA–water adduct, T–Si bonds do not show much elongation as

Table 1
Convergence of various geometrical parameters of T-BEA + H_2O as a function of plane wave cut-off.

Geometrical parameters	Sn-BEA	Sn-BEA + H_2O	Ti-BEA	Ti-BEA + H_2O
T–O Å (300 eV)	1.91	1.92	1.80	1.82
T–O Å (400 eV)	1.91	1.92	1.80	1.82
T–O Å (1000 eV)	1.91	1.92	1.80	1.82
T–Si Å (300 eV)	3.33	3.34	3.33	3.35
T–Si Å (400 eV)	3.33	3.36	3.33	3.36
T–Si Å (1000 eV)	3.33	3.36	3.33	3.36
T–O–Si deg. (300 eV)	143.0	145.9	152.0	157.8
T–O–Si deg. (400 eV)	143.0	145.2	152.0	157.7
T–O–Si deg. (1000 eV)	143.0	145.2	152.0	157.7
T–OH_2 Å (300 eV)	–	2.43	–	4.07
T–OH_2 Å (600 eV)	–	2.44	–	3.84
T–OH_2 Å (1000 eV)	–	2.44	–	3.84

compared to the bare T-BEA. For bare T-BEA, T–Si distance converges to 3.33 Å and for the corresponding adduct, it converges to 3.36 Å. T–O–Si bond angle gets much widened in the respective water adducts. For Sn-BEA and H_2O complex, the T–O–Si angle widens from 143° to 145.2°, where as for Ti-BEA it changes from 152° to 157.7°.

The most important inter-molecular interaction involves oxygen atom of water molecule with Sn- and Ti-atoms in BEA. In Sn-BEA, T–OH_2 distance varies from 2.43 Å to 2.44 Å, showing its convergence from 500 eV. However, in Ti-BEA, T–OH_2 distance varies from 3.84 Å to 4.13 Å and converges to 3.84 Å at 600 eV cut-off. Thus, the structural convergence is less sensitive to the number of PW and the evidence of this fact is given through Fig. 3. Fig. 3 represents the variation of Ewald energy i. e. nuclear–nuclear repulsion energy for Ti-BEA over the plane wave basis. This figure depicts the model plot of nuclear repulsion energy as a function of cut-off as rest of the systems follow similar trend. The Ewald energy plot (Fig. 3) distinctly shows a plateau around 600 eV cut-off. This leads to conclusion that the nuclear positions are fixed at and above these cut-offs. However, for low cut-offs of 400 eV and 500 eV, the difference of repulsion energy from converged energies is negligible and hence one can assume the qualitative structural convergence even at 500 eV. Thus, the convergence of the structural parameters at lower PW cut-off validates the use of ultrasoft pseudo-potentials. These results certainly indicate that for accurate structure one does not need very high kinetic energy cut-offs.

The convergence of adsorption energies with respect to the PW cut-offs for zeolitic system is one of the most crucial issues to be investigated. These catalytic materials are expected to exhibit the hydrophobic nature as water present is responsible in poisoning the active site. Discrepancy in calculation of the adsorption energy of water molecule on Sn- and Ti-BEA zeolite is already reported by us in our earlier study [34]. We next analyze the convergence of total energy and the desired properties dependent on it as a function of plane wave cut-off. Figs. 4 and 5a and b present the convergence of total energies of water and T-BEA systems, respectively. Fig. 6a and b depicts the interaction energies at variable cut-off for two different T-BEA systems with water molecule.

In our study of T-BEA and their weakly interacting water adduct, we attempt to determine properties that are essentially chemical in nature. Chemical properties are mostly determined by the electronic structure in the region between atoms, rather than in the space within atomic cores. This fact has already been made use of in the pseudo-potential approximation, and as we will see, it does not allow us to use a lower PW cut-off for the electronic energy convergence. The electronic energy is much more sensitive to the variation of PW cut-off. The total energy convergence of Ti-BEA–H_2O and Sn-BEA as a function of PW basis are plotted in Fig. 5a and b (rest of the systems follow a similar trend). The total energies of T-BEA and their respective water complexes are seen to converge very slowly at lower cut-offs up to 500 eV. At these cut-offs the difference in total energy is around 1 eV between two successive cut-offs. However, 600 eV onwards, this difference reduces and the total energies of all systems converge much faster. Absolute convergence can be seen from 900 eV to 1000 eV cut-off. For water molecule (see Fig. 4), although the convergence is relatively faster even at lower cut-offs, we observe that at cut-offs beyond 700 eV, the electronic energy is well saturated. The total energy decreases linearly up to 700 eV cut-off, beyond which a smooth convergence is observed. Although a solid is known to converge at a faster rate than the gas phase molecules, Fig. 4 shows a reverse trend. The electronic energy of molecular water converges at a lower cut-off of 600 eV. However, the interaction energy (defined as $E_{T-BEA+1H_2O} - (E_{T-BEA} + E_{1H_2O})$) which is a relative term, converges only at cut-offs larger than 800 eV. The oscillatory behavior of

interaction energy (Fig. 6a and b) affirms the failure of low cut-offs in calculating the energy-dependent properties. Interaction energy greatly fluctuates for low PW cut-off: 300–700 eV. At the cut-off 300 eV, the interaction energy values are clearly misleading, since Ti-BEA turns out to be more hydrophilic in nature compared to Sn-BEA. Several experimental and theoretical work [34,45] reports Sn-BEA to be strongly acidic and hydrophilic in nature. The variation in the convergence of interaction energy remains same even though the number of plane waves are increased. Thus, the evaluation of a relative property, such as the interaction energy, justifies role of exceptionally high cut-off in an energy-dependent property convergence.

A keen observation of Figs. 5a– 6b highlights a slight error in the convergence of total and interaction energies above 1000 eV cut-off. A good convergence of energies, absolute or interactive, is obtained up to 1000 eV, beyond which these values violate the convergence pattern. In this case, as already described in the computational discussion, when the cut-off reaches its high limiting value a denser grid construction is advisable to accommodate this exceeded threshold of PW.

Highest occupied molecular orbital (HOMO) and lowest unoccupied molecular orbital (LUMO) are characteristic of a particular system and are considered as the descriptors of global reactivity. Hence, for both individual T-BEA systems and their water adducts, we inspect the convergence of HOMO and LUMO with respect to the cut-off. HOMO, LUMO energies and their energy gap start to converge above 600 eV cut-off. For Sn-BEA, the converged values of HOMO and LUMO are -3.109 eV and 1.344 eV, respectively. For Ti-BEA, the HOMO converges to -3.144 eV and LUMO to 1.374 eV. For Sn-BEA adduct, the converged values of HOMO and LUMO are -2.891 eV and 1.659 eV, respectively. For Ti-BEA, adduct the corresponding values are -2.888 eV and 1.366 eV, respectively.

Analysis of HOMO orbital (figure not shown) at 500 eV and 1000 eV shows a contribution from the framework oxygen (clearly showing p-orbital lobes) surrounding the T-atom. The oxygen of water molecule does not contribute to the HOMO. Analysis of the LUMO orbital (figure not shown) at 500 eV and 1000 eV highlights the polarization of the neighboring framework oxygen due to T-atoms. The LUMO is mostly concentrated on the T-atom. In addition, the density on the oxygen atom of the water molecule is also polarized due to the T-atom. This is a most important outcome where a weak hydrogen bonding is observed between the framework oxygens (surrounding T-atom) and the H atom of the adsorbed water molecule. However, interestingly, we note that both the HOMO and LUMO orbital contour maps are converged by 500 eV cut-off, indicating that a lower cut-off is sufficient for studying the orbital contributions.

As an extension to this, we also evaluate a property, Electron Localization Function (ELF), which is often used to study the bonding pattern within molecules and solids [46,47]. Typically, the existence of an isosurface in the bonding region between two atoms at high values of ELF e.g. greater than 0.70 signifies a localized bonding. ELF is a function of $\rho(r)$ and hence $\psi(r)$. ELF contours (figure not shown) for a isovalue of 0.80 clearly show localized electron density around the oxygen atoms coming from the lone pair of electrons on them. The basins on the water molecule are merged showing them to be strongly covalent in nature. In contrast, the basins in zeolite cages are not merged. Around an isovalue of 0.65, the basins in the zeolite cage also merge. The ELF contours converge for a plane wave cut-off of 500 eV indicating that structural and electron densities converge earlier than the total energy values. Hence, we state explicitly that density-dependent properties along with structure converge at much lower cut-offs.

In addition, variation of unit cell parameters i.e. a, b, c is also studied as a function of cut-off. For both T-BEA systems, a, b and c converge to 12.66 Å, 12.66 Å and 26.29 Å, respectively, above

600 eV cut-off. Unlike geometrical features, lattice vectors are very sensitive to the quality of plane wave cut-off chosen. All the above values describing geometrical data match very well with our earlier electronic structure studies [34]. Thus, although the pseudo-potential techniques are easy to be applied for large complex systems, the evaluation of several properties, as described above, necessitates the need of proper selection of parameters like kinetic energy cut-off for the plane wave basis in their accurate description.

5. Conclusion

In this Letter, we study the role of a simple parameter, cut-off energy of a plane wave basis, required for an accurate description of periodic systems. Different types of bonding (intra- and inter-molecular) can be described with reasonable accuracy by a low plane wave cut-off. This fact is proved by the description of ELF and HOMO–LUMO contours. However, the total energy and relative properties depending on it, such as interaction energy, require a cut-off which is larger than that required for structural convergence. The role of plane wave basis extension for these periodic solids is exactly the same as that reported in earlier studies [11,48,49] for finite molecular systems. Hence, for these particular periodic systems one can use 500 eV cut-off in structural convergence, where as total energy convergence requires more than 800 eV cut-off.

We conclude that caution must be exercised while choosing these control parameters, both from the structural and energetic point of view, for systems involving ionic and weak interactions. Also, as discussed in the methodology, in order to avoid artificial results, additional parameters like grid size need to be set up properly.

References

[1] I.N. Levine, Quantum Chemistry, fourth edn., Prentice-Hall of India, 1995.
[2] P. Hohenberg, W. Kohn, Phys. Rev. B 140 (1964) 864.
[3] R.G. Parr, W. Yang, Density-functional Theory of Atoms and Molecules, Oxford University Press, 1989.
[4] M.C. Payne, M.P. Teter, D.C. Allan, T.A. Arias, J.D. Joannopoulos, Rev. Mod. Phys. 64 (1992) 1045.
[5] T.R. Cundari, M.T. Benson, M.L. Lutz, S.O. Sommerer, in: K.B. Lipkowitz, D.B. Boyd (Eds.), Reviews in Computational Chemistry, vol. 8, VCH, New York, 1996, p. 145.
[6] X. Gonze et al., Comput. Mater. Sci. 25 (2002) 478.
[7] M.D. Segall, P.J.D. Lindan, M.J. Probert, C.J. Pickard, P.J. Hasnip, S.J. Clark, M.C. Payne, J. Phys.: Condens. Matter 14 (2002) 2717.
[8] D. Marx, J. Hutter, Modern Methods and Algorithms of Quantum Chemistry, NIC, FZ, Julich, 2000. p. 301;
W. Andreoni, A. Curioni, Parallel Comput. 26 (2000) 819.
[9] G. Kresse, J. Hafner, Phys. Rev. B 48 (1993) 13115.
[10] G. Kresse, J. Furthermuller, Comput. Mater. Sci. 6 (1996) 15.
[11] C. Raynaud, L. Maron, F. Jolibois, J.-P. Daudey, P.M. Esteves, A. Ramírez-Solís, Chem. Phys. Lett. 414 (2005) 161.
[12] K. Lee, J. Yu, Y. Morikawa, Phys. Rev. B 75 (2007) 45402.
[13] T. Todorova, A.P. Seitsonen, J. Hutter, I.W. Kuo, C.J. Mundy, J. Phys. Chem. B 110 (2006) 3685.
[14] J. Paier, R. Hirschl, M. Marsman, G. Kresse, J. Chem. Phys. 122 (2005) 234102.
[15] S. Casassa, M. Catalayud, K. Doll, C. Minot, C. Pisani, Chem. Phys. Lett. 409 (2005) 110.
[16] G. Festa, M. Cossi, V. Barone, G. Cantele, D. Ninno, G. Iadonisi, J. Chem. Phys. 122 (2005) 184714.
[17] C. Janfelt, F. Jensen, Chem. Phys. Lett. 406 (2005) 501.
[18] A. Corma, J. Catal. 216 (2003) 298.

[19] J. Stelzer, M. Paulus, M. Hunger, J. Weitkamp, Micropor. Mesopor. Mater. 22 (1998) 1.
[20] M. Boronat, A. Corma, M. Renz, G. Sastre, P.M. Viruela, Chem. Eur. J. 11 (2005) 6905.
[21] M. Boronat, A. Corma, M. Renz, R.M. Viruela, Chem. Eur. J. 12 (2006) 7076.
[22] S. Shetty, S. Pal, D.G. Kanhere, A. Goursot, Chem. Eur. J. 12 (2006) 518.
[23] R.L. Wadlinger, G.T. Kerr, E.J. Rosinski, US Patent (1967) 3308069.
[24] V.A. Tuan, S. Li, R.D. Noble, J.L. Falconer, Environ. Sci. Technol. 37 (2003) 4007.
[25] J.C. van der Waal, H. van Bekkum, J. Mol. Catal. 124 (1997) 137.
[26] A. Carati, C. Flego, P. Massara, R. Millini, L. Carluccio, W.O. Parker Jr., G. Bellussi, Microporous. Mesoporous. Mater. 30 (1999) 137.
[27] R.J. Saxton, J.G. Zajacek, G.L. Crocco, Zeolites 17 (1996) 315.
[28] T. Blasco, M.A. Camblor, A. Corma, Peârez-Pariente, Am. Chem. Soc. 115 (1993) 11806.
[29] A. Corma, M.E. Domine, J.A. Gaona, M.T. Navarro, F. Rey, S. Valencia, Stud. Surf. Sci. Catal. 135 (2001) 1812.
[30] N.K. Mal, A.V. Ramaswamy, Chem. Commun. 425 (1997).
[31] A. Corma, L.T. Nemeth, M. Renz, S. Valencia, Nature 412 (2001) 423.
[32] G. Sastre, A. Corma, Chem. Phys. Lett. 302 (1999) 447.
[33] S.R. Bare et al., J. Am. Chem. Soc. 127 (2005) 12924.
[34] S. Shetty, B.S. Kulkarni, S. Pal, D.G. Kanhere, A. Goursot, J. Phys. Chem. B 112 (2008) 2573.
[35] A.J.M. de Man, J. Sauer, J. Phys. Chem. 100 (1996) 5025.
[36] S. Krishnamurty, S. Pal, A. Goursot, R. Vetrivel, Microporous. Mesoporous. Mater. 48 (2001) 383.
[37] S. Krishnamurty, S. Pal, J. Phys. Chem. A 104 (2000) 7639.
[38] J. Sauer, Chem. Rev. 89 (1989) 199.
[39] C. Pisani, R. Dovesi, C. Roetti, C. Hartree-Fock, Ab Initio Treatment of Crystalline Systems, Springer-Verlag, Berlin, 1988.
[40] E.H. Teunissen et al., R. Simul. Mater. Sci. Eng. 2 (1994) 921.
[41] X. Rozanska, Th. Demuth, F. Hutschka, J. Hafner, R.A. van Santen, J. Phys. Chem. B 106 (2002) 3248.
[42] J.M. Newsam, M.M.J. Treacy, W.T. Koetsier, C.B. de Gruyter, Proc. R. Soc. London, A 420 (1988) 375.
[43] D. Vanderbilt, Phys. Rev. B 41 (1990) 7892.
[44] J.P. Perdew, Y. Wang, Phys. Rev. B 45 (1992) 13244.
[45] A. Corma, M.E. Domine, S. Valencia, J. Catal. 215 (2003) 294.
[46] S. Krishnamurty, S. Chacko, D.G. Kanhere, G.A. Breaux, C.M. Neal, M.F. Jarrold, Phys. Rev. B 73 (2006) 045406.
[47] B. Silvi, A. Savin, Nature (London) 371 (1994) 683.
[48] F.C.E. Byrd, G.E. Scuseria, C.F. Chabalowski, J. Phys. Chem. B 108 (2004) 13100.
[49] S. Tosoni, C. Tuma, J. Sauer, B. Civalleri, P. Ugliengo, J. Chem. Phys. 127 (2007) 154102.